Published OnlineFirst January 15, 2014; DOI: 10.1158/1078-0432.CCR-13-2235

Cancer Therapy: Clinical

Clinical Cancer Research

A Phase I, Pharmacokinetic, and Pharmacodynamic Study of Panobinostat, an HDAC Inhibitor, Combined with Erlotinib in Patients with Advanced Aerodigestive Tract Tumors

Jhanelle E. Gray[1,4], Eric Haura[1,4], Alberto Chiappori[1,4], Tawee Tanvetyanon[1], Charles C. Williams[1], Mary Pinder-Schenck[1,4], Julie A. Kish[2], Jenny Kreahling[4], Richard Lush[4,5], Anthony Neuger[4,5], Leticia Tetteh[3], Angela Akar[1], Xiuhua Zhao[6], Michael J. Schell[6], Gerold Bepler[7], and Soner Altiok[4]

Abstract

Purpose: Panobinostat, a histone deacetylase (HDAC) inhibitor, enhances antiproliferative activity in non–small cell lung cancer (NSCLC) cell lines when combined with erlotinib. We evaluated this combination in patients with advanced NSCLC and head and neck cancer.

Experimental Design: Eligible patients were enrolled in a 3+3 dose-escalation design to determine the maximum tolerated dose (MTD) of twice weekly panobinostat plus daily erlotinib at four planned dose levels (DL). Pharmacokinetics, blood, fat pad biopsies (FPB) for histone acetylation, and paired pre and posttherapy tumor biopsies for checkpoint kinase 1 (CHK1) expression were assessed.

Results: Of 42 enrolled patients, 33 were evaluable for efficacy. Dose-limiting toxicities were prolonged-QTc and nausea at DL3. Adverse events included fatigue and nausea (grades 1–3), and rash and anorexia (grades 1–2). Disease control rates were 54% for NSCLC ($n = 26$) and 43% for head and neck cancer ($n = 7$). Of 7 patients with NSCLC with EGF receptor (*EGFR*) mutations, 3 had partial response, 3 had stable disease, and 1 progressed. For *EGFR*-mutant versus *EGFR* wild-type patients, progression-free survival (PFS) was 4.7 versus 1.9 months ($P = 0.43$) and overall survival was 41 (estimated) versus 5.2 months ($P = 0.39$). Erlotinib pharmacokinetics was not significantly affected. Correlative studies confirmed panobinostat's pharmacodynamic effect in blood, FPB, and tumor samples. Low CHK1 expression levels correlated with PFS ($P = 0.006$) and response ($P = 0.02$).

Conclusions: We determined MTD at 30 mg (panobinostat) and 100 mg (erlotinib). Further studies are needed to further explore the benefits of HDAC inhibitors in patients with *EGFR*-mutant NSCLC, investigate FPB as a potential surrogate source for biomarker investigations, and validate CHK1's predictive role. *Clin Cancer Res; 20(6); 1644–55. ©2014 AACR.*

Introduction

The hypoacetylation of histones and key proteins, including oncogenes and tumor suppressor genes, plays an important role in carcinogenesis (1–3). Histone acetylation and deacetylation are tightly regulated by histone acetyltransferases and histone deacetylases (HDAC) in normal cells. However, in tumor cells, this process can be aberrant (4, 5). The blockade of HDACs leads to silencing of transcription via repression of genes and chromatin condensation in many tumor types (3, 6, 7).

Panobinostat (LBH589), an oral pan-HDAC inhibitor, has demonstrated antitumor effects in preclinical studies (8–12), including in non–small cell lung cancer (NSCLC). In clinical trials, the main toxicities of panobinostat are diarrhea, nausea, and thrombocytopenia (13, 14). Previously, we showed that protein levels of checkpoint kinase 1 (CHK1), which has a major role in G_2 cell-cycle checkpoint regulation (15), was markedly reduced in lung cancer cells treated with pan- and selective HDAC inhibitors, including panobinostat (16), suggesting that CHK1 may be used as a pharmacodynamic marker to assess HDAC inhibitor efficacy in tumor tissue.

The EGF receptor (EGFR) is an important therapeutic target in upper aerodigestive tract tumors, including NSCLC and head and neck cancers. It impacts diverse oncogenic pathways that regulate cell proliferation, survival, and invasion (17). Erlotinib, an U.S. Food and Drug Administration (FDA)–approved EGFR tyrosine kinase inhibitor (TKI), has

Authors' Affiliations: Departments of [1]Thoracic Oncology, [2]Head and Neck Oncology, and [3]Cutaneous Oncology; [4]Chemical Biology and Molecular Medicine Program; [5]Clinical Pharmacology Core; [6]Biostatistics Core, H. Lee Moffitt Cancer Center and Research Institute, Tampa, Florida; and [7]Karmanos Cancer Institute, Detroit, Michigan

Prior presentation: Portions of the study were presented in preliminary abstract only form at the 2010 Annual Meeting of the American Society of Clinical Oncology, June 4–8, 2010, Chicago, IL.

Corresponding Author: Jhanelle E. Gray, H. Lee Moffitt Cancer Center and Research Institute, 12902 Magnolia Drive, FOB1, Tampa, FL 33612. Phone: 813-745-6895; Fax: 813-745-3027; E-mail: Jhanelle.Gray@moffitt.org

doi: 10.1158/1078-0432.CCR-13-2235

Published OnlineFirst January 15, 2014; DOI: 10.1158/1078-0432.CCR-13-2235

Translational Relevance

This study provides a detailed evaluation of the safety, toxicity, pharmacokinetics, and pharmacodynamics of panobinostat when combined with erlotinib in patients with non–small cell lung cancer (NSCLC) and head-and-neck cancer. While erlotinib 150 mg daily plus panobinostat at 30 mg twice weekly had dose-limiting toxicities, erlotinib 100 mg daily and panobinostat 30 mg twice weekly were generally well tolerated. Evaluation of pharmacodynamic markers obtained on serial tumor biopsies demonstrated that checkpoint kinase 1 (CHK1) expression significantly correlated with progression-free survival and tumor response. We also describe a novel approach to evaluating drug-mediated changes in histone acetylation in subcutaneous abdominal adipose tissue obtained via fine needle aspiration. Further evaluation of CHK1's predictive potential for efficacy assessment and the combination in a select NSCLC patient population should be considered. With more than 100 current studies evaluating histone deacetylase inhibitors, assessment of fat pad biopsies is relevant for future clinical trial investigations.

been shown to improve outcomes in previously treated patients with NSCLC, with a standard single-agent dose of 150 mg daily (18). In the preclinical setting, we and others have shown that HDAC inhibition, including with panobinostat, in *EGFR*-mutant, TKI-sensitive NSCLC cell lines results in depletion of EGFR and induction of apoptosis. In addition, these data suggest that the addition of panobinostat to erlotinib may not only enhance erlotinib efficacy but also overcome EGFR-TKI resistance (8, 19–23).

On the basis of the enhanced effects observed with erlotinib in combination with panobinostat in NSCLC cell lines (8, 19–21), we conducted a phase I study with expansion in patients with advanced NSCLC and with head and neck cancers. The objectives were to establish the safety and tolerability, to collect preliminary efficacy data, and to determine the pharmacokinetic and pharmacodynamic profiles in blood, paired tumor, peripheral blood mononuclear cells (PBMC), and fat pad biopsies (FPB).

Patients and Methods

The Institutional Review Board at the University of South Florida approved the protocol for this single-institution study (ClinicalTrials.gov identifier NCT00738751). Informed consent was obtained from all patients enrolled on the study. Patients were recruited from the thoracic oncology and head and neck clinics at the H. Lee Moffitt Cancer Center and Research Institute. Eligible patients included those $\geq$18 years of age with advanced/metastatic NSCLC or head and neck cancer who had failed at least one line of systemic therapy. Participants had measurable disease defined by Response Evaluation Criteria in Solid Tumors (RECIST; version 1.0), an Eastern Cooperative Oncology Group Performance Status $\leq$1, no prior systemic chemotherapy within 14 days, no cardiac dysfunction, and a baseline multi-gated acquisition scan or echocardiogram demonstrating a left ventricular ejection fraction equal to or above the lower limit of the institutionally normal value (50%). Patients with stable, asymptomatic pretreated brain metastases no longer requiring steroids were allowed. Potentially fertile participants had to agree to use an approved contraceptive method. Patients with significant laboratory abnormalities were excluded. There were no limits to number of prior therapies. Prior EGFR-TKI therapy was permitted.

Study design

This was a dual-agent, phase I study with an expansion arm (n = 20 patients) at the recommended phase II dose (RP2D). Eligible patients were enrolled at escalating dose levels of oral erlotinib in combination with oral panobinostat in a standard 3+3 design. The RP2D was defined as the highest dose level of panobinostat in combination with erlotinib that induced a dose-limiting toxicity (DLT) in fewer than 33% of patients. Cohorts of 3 to 6 eligible patients were treated with escalating doses of oral erlotinib and panobinostat oral capsules.

If a DLT occurred (see Safety and Efficacy Analyses below for definition), then 3 additional patients were entered at the same dose. If there were no more DLTs, dose escalation continued. Dose escalation was performed after all patients at the previous dose level completed 3 weeks of treatment. An additional 20 patients with NSCLC and head and neck cancer were treated at the RP2D level to characterize the toxicity profile, perform the biomarker analysis, and evaluate for preliminary antitumor activity.

Treatment delivery

Each cycle was defined as a 21-day period. Erlotinib was taken daily without interruption. Panobinostat was taken twice weekly, for 2 out of 3 weeks of each cycle. Four dose levels of panobinostat in combination with erlotinib were planned: (i) dose level 1 (DL1) = panobinostat 20 mg *per os* twice weekly for 2 out of 3 weeks + erlotinib 100 mg *per os* daily; (ii) dose level 2 (DL2) = panobinostat 30 mg and erlotinib 100 mg; (iii) dose level 3 (DL3) = panobinostat 30 mg and erlotinib 150 mg; and (iv) dose level 4 (DL4) = panobinostat 40 mg and erlotinib 150 mg. Doses were not escalated over the course of treatment of an individual patient.

Safety and efficacy analyses

Toxicities at baseline and on study were graded according to the Common Terminology Criteria for Adverse Events (version 3.0). DLT was defined as grade 4 rash, grade 3/4 nausea/vomiting refractory to anti-emetics, grade 3/4 diarrhea refractory to anti-diarrhea medications, QTc prolongation $\geq$500 milliseconds or >480 milliseconds on $\geq$2 occasions, other grade 3/4 nonhematologic toxicity, grade 4 hematologic toxicity, or treatment-related death occurring within cycle 1. Dose-modification guidelines for toxicity were available in the protocol. Treatment was continued until disease progression, unacceptable adverse effects, or

Published OnlineFirst January 15, 2014; DOI: 10.1158/1078-0432.CCR-13-2235

withdrawal of informed consent. Radiologic assessments were performed every two cycles. To determine tumor progression or response, RECIST version 1.0 was used.

Pharmacokinetic studies

Mandatory pharmacokinetic plasma sampling was performed on day 8 (erlotinib), day 9 (erlotinib and panobinostat), and day 15 (erlotinib and panobinostat) of cycle 1 at predose and at 0.5, 2, 4, 6, 8–10, and 24 hours postdose for all participants enrolled.

Plasma samples were collected and stored at −70°C until analysis. Methods for quantitation and pharmacokinetic analysis of erlotinib (24, 25) and panobinostat (26) have been previously published. The disposition of erlotinib in the presence of panobinostat (days 9 and 15) was compared with that shown in the absence of panobinostat (day 8).

Correlative studies

EGFR mutation analyses were performed on all patients with NSCLC by direct sequencing of exons 18 to 21 in a Clinical Laboratory Improvement Amendments (CLIA)-certified laboratory using available tumor specimens; a dedicated tumor biopsy before study enrollment for mutation assessment was not required.

All patients enrolled had pre and posttreatment blood draws and subcutaneous adipose tissue sampling for histone acetylation. In addition, in those who consented, optional pretreatment and C1D18 ± 7 tumor biopsies under image guidance by a board-certified cytopathologist were obtained for correlative studies.

For immunohistochemical analyses, tumor slides were stained with E-cadherin (Cell Marque Corporation; 760-4440), CHK1 (Abcam; ab47574), or acetylated α-tubulin (Abcam; ab24610) antibodies using a Ventana Discovery XT automated system (Ventana Medical Systems) as per the manufacturer's protocol with proprietary reagents. The Allred scoring system was used to evaluate the percentage of positive stained cells and staining intensity (27). A proportion score was assigned representing the proportion of positively stained tumor cells (0 = none; 1 = <1/100; 2 = 1/100 to <1/10; 3 = 1/10 to 1/3; 4 = 1/3 to 2/3; and 5 = >2/3). Average intensity of staining in positive cells was assigned as an intensity score (0 = none; 1 = weak; 2 = intermediate; and 3 = strong). Proportion score and intensity score were added to obtain a total score ranging from 0 to 8. Briefly, histone acetylation was assessed in FPB and in PBMCs by Western blot analysis using acetyl-histone H4 (Cell Signaling Technology; 2591S) and β-actin (Sigma; A1978) antibodies, as previously described (16); β-actin was used as a loading control.

Statistical analysis

Efficacy analyses were performed in both efficacy evaluable patients (defined as those who completed at least 75% of cycle 1 of the combination treatment) and the intent-to-treat patients. Median survival for patients who were *EGFR*-mutant was estimated assuming an exponential survival distribution. Progression-free survival (PFS) and overall survival (OS) times were estimated using Kaplan–Meier curves. Survival comparisons between the *EGFR*-mutant group and the other patient groups were performed using the log-rank test. Efficacy comparisons for response were performed using the Mantel–Haenszel test. Correlations with Allred scores were assessed using Spearman correlation. A P value of <0.05 was considered statistically significant. All analyses used SAS version 9.3.

Results

Patients and treatment

Forty-two patients were enrolled (3, 8, and 7 at consecutive dose levels and 24 at the RP2D, with all evaluable for toxicity and 33 evaluable for efficacy analyses) from January 2009 until February 2011. Table 1 summarizes patient characteristics. Reasons for patients being nonevaluable for efficacy included rapid clinical progression ($n = 3$), patient withdrawal ($n = 3$), adverse events not related to panobinostat or erlotinib ($n = 1$), and serious adverse events related to study therapy ($n = 2$; DLT). The median number of cycles received for patients at DL1, DL2, and DL3 and across all patients enrolled was 1, 1.5, 1, and 2 (maximum 35), respectively. Nine patients received six or more cycles of treatment. Four of the 8 patients with *EGFR* mutation had prior erlotinib treatment. The maximum tolerated dose (MTD) and the RP2D were defined as oral erlotinib 100 mg daily and panobinostat 30 mg twice weekly for 2 weeks of the 21-day cycle. No patient received drugs at DL4.

Table 1. Summary of patient characteristics ($N = 42$)

Characteristic	No. of patients	Percentage
Age, y		
Mean	60.8	
Range	47–78	
Gender		
Female	23	55
Male	19	45
Histology		
NSCLC		
Adenocarcinoma	25	60
Squamous cell carcinoma	8	19
Neuroendocrine carcinoma	1	2
Adenosquamous cell carcinoma	1	2
Head and neck	7	17
EGFR status—lung adenocarcinoma		
Mutant	8	32
Wild-type	9	36
Unknown	8	32
Mean number of prior regimens	2.3	
Smoking status		
Current	4	9
Former	31	74
Never	7	17
Prior erlotinib	9	21

Published OnlineFirst January 15, 2014; DOI: 10.1158/1078-0432.CCR-13-2235

Table 2. Treatment-related, grade 2 or greater toxicities[a]

	DL1: erlotinib 100 mg + panobinostat 20 mg (grade)			DL2: erlotinib 100 mg + panobinostat 30 mg (grade)			DL3: erlotinib 150 mg + panobinostat 30 mg (grade)			Dose expansion (grade)			
Adverse event	**2**	**3**	**4**	**2**	**3**	**4**	**2**	**3**	**4**	**2**	**3**	**4**	**Total**
Albumin, serum low (hypoalbuminemia)										1			**1**
Anorexia	1						3			5			**9**
Atrial fibrillation											1		**1**
Constipation										1			**1**
Cough										1			**1**
Dehydration	1			1						1			**3**
Diarrhea				1			1			3			**5**
Dyspnea (shortness of breath)							1			5	1		**7**
Fatigue (asthenia, lethargy, malaise)	1			2			5			9	3		**20**
Gastrointestinal/gastroesophageal reflux disease/gastritis										3			**3**
Glucose, serum-high (hyperglycemia)							1						**1**
Hair loss/alopecia (scalp or body)							1						**1**
Hemoglobin	1									1			**2**
Hypertension										1			**1**
Infection	2												**2**
Leukocytes (total white blood count)										1			**1**
Lymphopenia	1		1								1		**3**
Mood alteration—anxiety										1			**1**
Muscle weakness				1									**1**
Mucositis/stomatitis		1					1			1			**3**
Nausea							1	1					**2**
Neuropathy: sensory		1											**1**
Neutrophils/granulocytes (ANC/AGC)					1								**1**
Pain	2			1						3			**6**
Phosphate, serum low (hypophosphatemia)										1			**1**
Platelets		1						1		2	5		**9**
Prolonged QTc interval								1					**1**
PTT (partial thromboplastin time)											1		**1**
Rash/desquamation/pruritus	2			5			2			5			**14**
Rigors/chills	1												**1**
Thyroid function, low (hypothyroidism)										3			**3**
Vomiting	1			1			1			2			**5**
Weight loss	2												**2**
Totals	**15**	**3**	**1**	**12**	**1**	**0**	**17**	**3**	**0**	**50**	**12**	**0**	**114**

NOTE: The bold was used to make totals stand out.

[a]Occurring in greater than 10% of patients. Grand totals across all grades: grade 2 was 94, grade 3 was 19, and grade 4 was 1.

Toxicity

In the DL1 group, no DLTs occurred in 3 evaluable patients. At DL2, 1 of the 6 evaluable patients experienced grade 3 atrial fibrillation, although the episode occurred during an albuterol nebulizer treatment. At DL3, two DLTs occurred in the 5 patients enrolled (grade 3 nausea and grade 3 prolonged QTc). All DLTs resolved with cessation of the study agents, and no permanent sequelae were observed.

There were 583 separate adverse events recorded that were possibly, probably, or definitely related to study therapy (431, 122, 29, and 1 for grades 1, 2, 3, and 4, respectively). The most common adverse events were fatigue and nausea (grades 1–3) and rash and anorexia (grades 1–2). Dose reductions were required for thrombocytopenia ($n = 1$) and nausea ($n = 1$). Table 2 provides an overview of treatment-related, grade 2, or higher adverse events occurring in >10% of the patients. No patients died while on active treatment. Two patients died during their 30-day follow-up period from complications not felt to be related to study drug. One died of chronic obstructive pulmonary disease exacerbated by

Published OnlineFirst January 15, 2014; DOI: 10.1158/1078-0432.CCR-13-2235

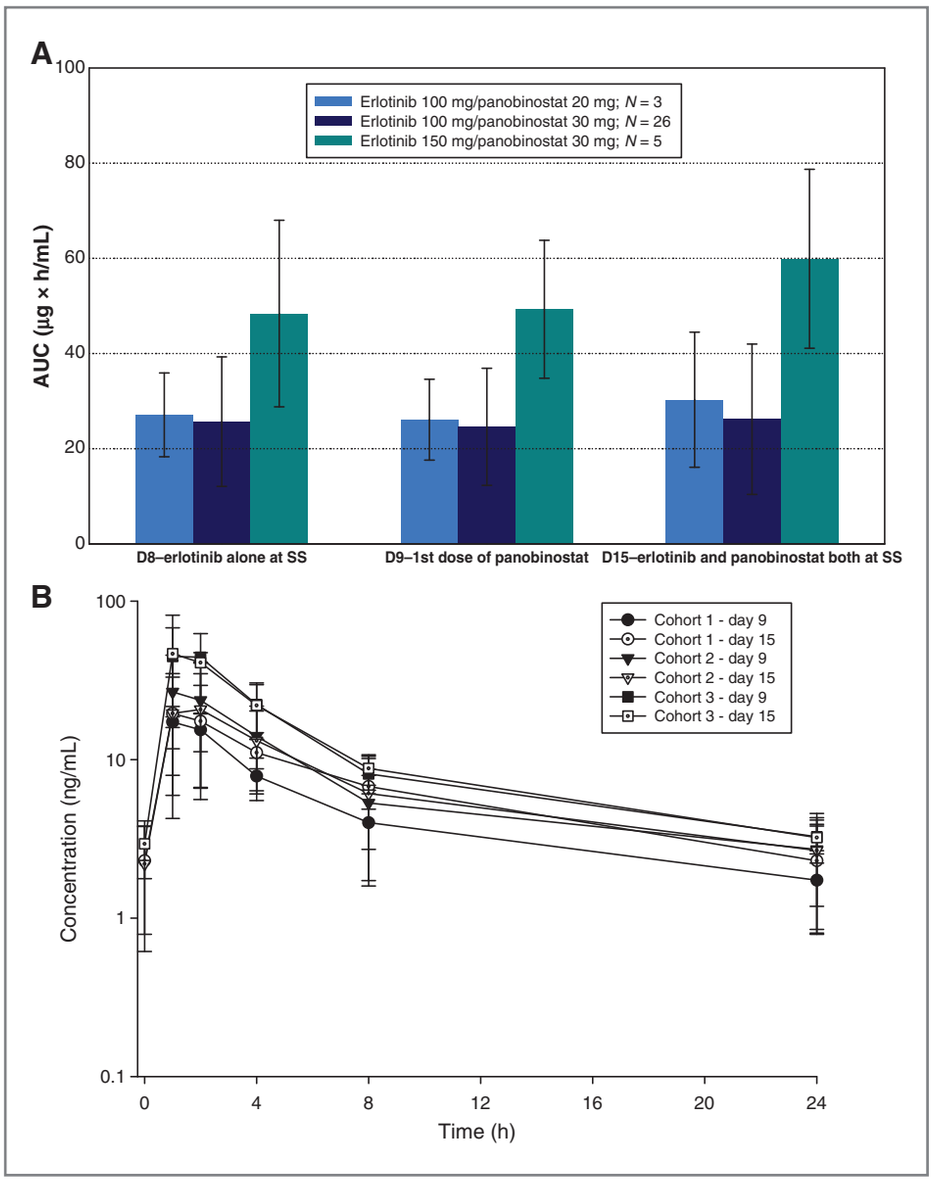

Figure 1. Pharmacokinetic analyses. A, erlotinib exposure ($AUC_{0–24\ h}$) with and without the presence of panobinostat in the dose-escalation cohorts. Includes only those patients who completed all 3 days of pharmacokinetic blood draws. B, panobinostat time versus mean plasma concentration (± SD) in the dose-escalation cohorts. Includes only those patients who completed all 3 days of pharmacokinetic blood draws. SS, steady state.

multiple pulmonary emboli and the other from a myocardial infarction possibly triggered by direct tumor extension.

Pharmacokinetic studies

Area under the curve (AUC) was calculated for erlotinib at steady state on day 8, at first exposure to panobinostat on day 9, and when both drugs were at steady state on day 15. During each evaluated day, the AUC for erlotinib was proportional to dose. The dosing of panobinostat did not significantly affect the pharmacokinetics of erlotinib (Fig. 1A and B).

Efficacy analyses

Of 42 patients enrolled, 33 were evaluable for response (Fig. 2). One patient who experienced a DLT (prolonged QTc) was not included in the efficacy assessments, as the patient did not complete at least 75% of cycle 1. When we combined patients regardless of tumor type or histology, we found that there were 3 (9%) partial responses (PR) and 14 (42%) patients with stable disease; disease control rate (DCR) was 52%.

By histology. By tumor type, the DCR was 54% for NSCLC ($n = 26$) and 43% for head and neck cancer ($n = 7$). By histology for those with NSCLC, the adenocarcinoma ($n = 18$) versus squamous cell lung cancer (SQCLC; $n = 7$) patients had a better response profile: 3 (17%) versus 0 (0%) with PR, 10 (55%) versus 1 (14%) with stable disease, and 5 (28%) versus 6 (86%) with progressive disease, respectively ($P = 0.015$). One additional patient with neuroendocrine lung cancer had progressive disease. Among the 7 patients with head and neck cancer, 3 (43%) achieved stable disease and 4 (57%) progressed. Of the 17 participants who went

Published OnlineFirst January 15, 2014; DOI: 10.1158/1078-0432.CCR-13-2235

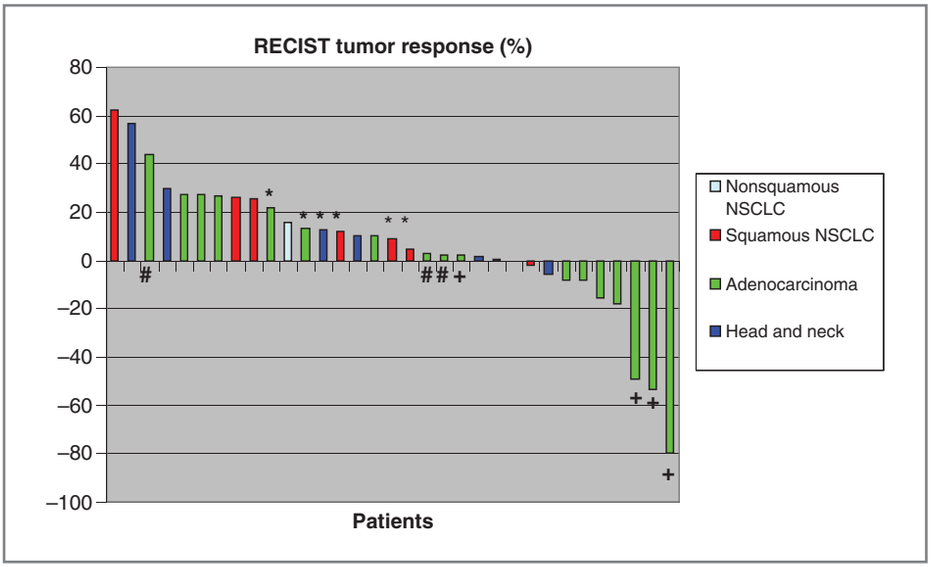

Figure 2. Best percentage change in target lesions based on RECIST v1.0. +, Erlotinib-naïve, *EGFR* mutant; #, EGFR mutant with prior erlotinib exposure; *, progressive disease based on new lesions.

on to receive further treatment, 1 was nonevaluable, 4 achieved a PR (subsequent therapies included carboplatin plus paclitaxel, pemetrexed, and docetaxel), 4 had progressive disease, and 8 had stable disease to subsequent therapies.

EGFR mutant. A total of 7 evaluable patients had *EGFR* mutations; all had adenocarcinoma of the lung. The three PRs achieved at the RP2D occurred in patients with an exon 21 *EGFR* mutations (L858R) who were EGFR-TKI naive. Two of these patients remained on therapy for more than 30 cycles. In the remaining patients with lung adenocarcinoma with *EGFR* mutations ($n = 7$ total), 3 had stable disease [1 was EGFR-TKI naïve with exon 20 mutation (T785T) and exon 21 (L858R)], 2 had prior EGFR-TKI exposure [with 1 having a point mutation in exon 18 (G719A) and another with an exon 19 deletion], and 1 progressed [had prior EGFR-TKI exposure and *EGFR* exon 21 mutation (L858R)]. In summary, 3 *EGFR*-mutant patients had prior erlotinib exposure, with a median time between erlotinib treatments of 3 months (range, 14 days to 1.5 years), whereas their prior duration of erlotinib treatment ranged from 1 to 3.5 years. Of the 10 patients with lung adenocarcinoma with stable disease, 5 patients had prior exposure to erlotinib for $\geq$3 months. One patient with an *EGFR* exon 19 deletion, who was initiated on study within 3 months after having documented progression following 1 year of erlotinib plus bevacizumab, achieved stable disease on study for 10 cycles.

EGFR wild-type. Seven evaluable patients were identified with *EGFR* wild-type NSCLC: 5 (72%) patients had stable disease (all adenocarcinoma, with 2 having prior EGFR-TKI exposure), and 2 (28%) patients had progressive disease (1 with adenocarcinoma and prior EGFR-TKI exposure, and 1 with SQCLC). Of the 3 *EGFR* wild-type patients with prior EGFR-TKI exposure, 1 patient with stable disease had an 18% reduction in tumor burden by RECIST. This patient was a lifetime never-smoker with lung adenocarcinoma who had been previously treated with erlotinib for 2 years, with the first year receiving a combination treatment with bevacizumab. This patient enrolled on study at time of overt radiographic progression and remained on treatment for 11 cycles until development of intolerable nausea. Repeat molecular testing performed confirmed the prior results of *EGFR* wild-type and noted that the patient did not harbor any detectable abnormalities in *KRAS*, *ALK*, *BRAF*, or *PI3K*.

Although the numbers are small, we present some comparisons here among those with known *EGFR* status and eligible for the efficacy analyses. The DCRs were similar for *EGFR*-mutant (85%; $n = 7$) and *EGFR* wild-type patients (71%; $n = 7$).

EGFR-TKI naïve versus prior exposure. Of the 26 patients with NSCLC evaluable for efficacy, 7 patients with lung adenocarcinoma had prior EGFR-TKI exposure, whereas 19 patients with NSCLC (11 adenocarcinoma, 7 SQCLC, and 1 neuroendocrine) did not. Of the 14 patients with NSCLC with known *EGFR* mutation status, 6 had prior EGFR-TKI exposure and 8 were EGFR-TKI naïve. Among the 7 patients with an *EGFR* mutation, 2 of the 3 EGFR-TKI–exposed patients were nonprogressors compared with 4 of 4 EGFR-TKI–naïve patients. In the 7 *EGFR* wild-type patients, 2 of 3 EGFR-TKI–exposed were nonprogressors compared with 3 of 4 EGFR-TKI–naïve patients. Of the 12 patients with NSCLC with unknown *EGFR* status, the one patient (mentioned above) with prior EGFR-TKI exposure had stable disease, whereas 2 of the 11 EGFR-TKI–naïve patients were nonprogressors. None of the 7 patients with head and neck cancer had prior EGFR-TKI exposure.

Of those 7 patients with prior EGFR-TKI exposure, their course on study was reviewed. One patient was removed for toxicity; 1 patient withdrew consent; 3 patients developed slow progression over a time of at least six cycles (2 of the 3 were *EGFR* mutant), whereas 2 patients developed rapid progression within the first two cycles (1 was *EGFR* mutant).

Published OnlineFirst January 15, 2014; DOI: 10.1158/1078-0432.CCR-13-2235

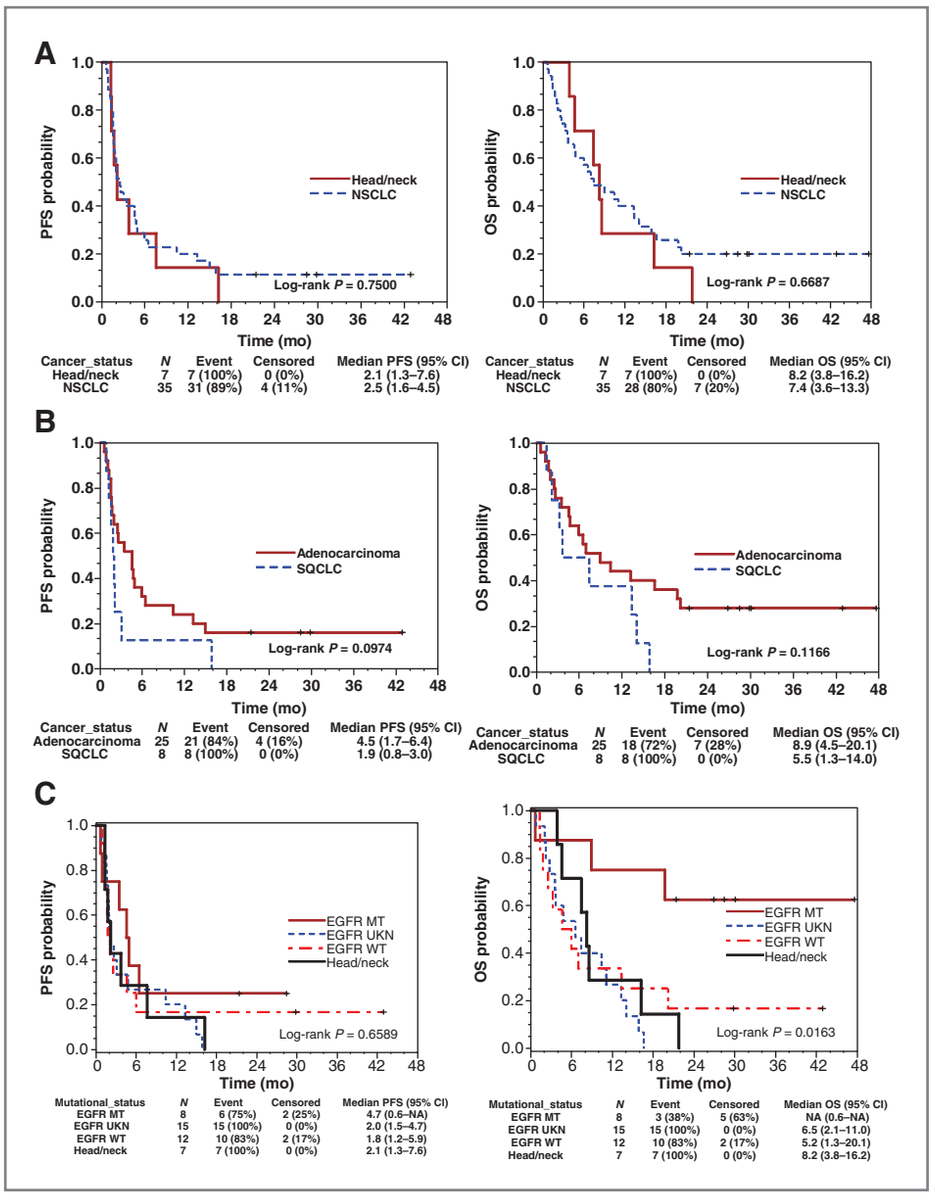

Figure 3. PFS and OS for the intent-to-treat population. A, no difference in PFS or OS for patients with NSCLC versus head and neck cancer. B, excluding the patients with head and neck cancer (see Table 1 for number of patients), when comparing SQCLC versus non-SQCLC, no significant differences in PFS or OS were observed. C, OS was not yet reached for the EGFR-mutant NSCLC group but in a *post hoc* analysis was estimated to be 41 months ($P = 0.0087$) compared with the other groups. EGFR+, *EGFR* mutant adenocarcinoma of the lung; EGFR−, *EGFR* wild-type NSCLC; Head/neck, head and neck cancer; Unknown, *EGFR* mutation status unknown; CI, confidence interval.

PFS and OS. In the intent-to-treat population ($n = 42$), PFS and OS curves are presented in Fig. 3. For the patients with NSCLC and head and neck cancer, median OS was 7.4 versus 8.2 months ($P = 0.67$) and median PFS was 2.5 versus 2.1 months ($P = 0.75$), respectively (Fig. 3A). For patients with NSCLC with adenocarcinoma versus SQCLC, median PFS was 4.5 months versus 1.9 months ($P = 0.10$) and OS was 8.9 versus 5.5 months ($P = 0.12$), respectively (Fig. 3B). The PFS and OS results across the four groups (NSCLC: *EGFR*-mutant, *EGFR* wild-type, and *EGFR* unknown lung cancers; head and neck cancer) are presented in Fig. 3C. Assuming survival to follow an exponential distribution, the estimated median OS for the 8 *EGFR*-mutant patients was 41 months, compared with at most 8.2 months for the other subgroups. Five of the 8 known *EGFR*-mutant patients were still alive at ≥21 months. When patients with head and neck cancer are removed from Fig. 3C, leaving only the 35 patients with NSCLC, in three subgroups the PFS is not significant ($P = 0.43$), whereas the OS remains significantly different ($P = 0.039$; data not shown). It is notable that, although 3 of the 6 *EGFR*-mutant patients who ultimately progressed remain alive, all 25 with progression from the *EGFR* wild-type and unknown groups have died ($P = 0.0003$).

CHK1 expression inversely correlates with E-cadherin expression and tumor response to panobinostat and erlotinib therapy

G2–M cell-cycle checkpoint regulators, including CHK1 and CDC2, play an important role in HDAC inhibitor–

Published OnlineFirst January 15, 2014; DOI: 10.1158/1078-0432.CCR-13-2235

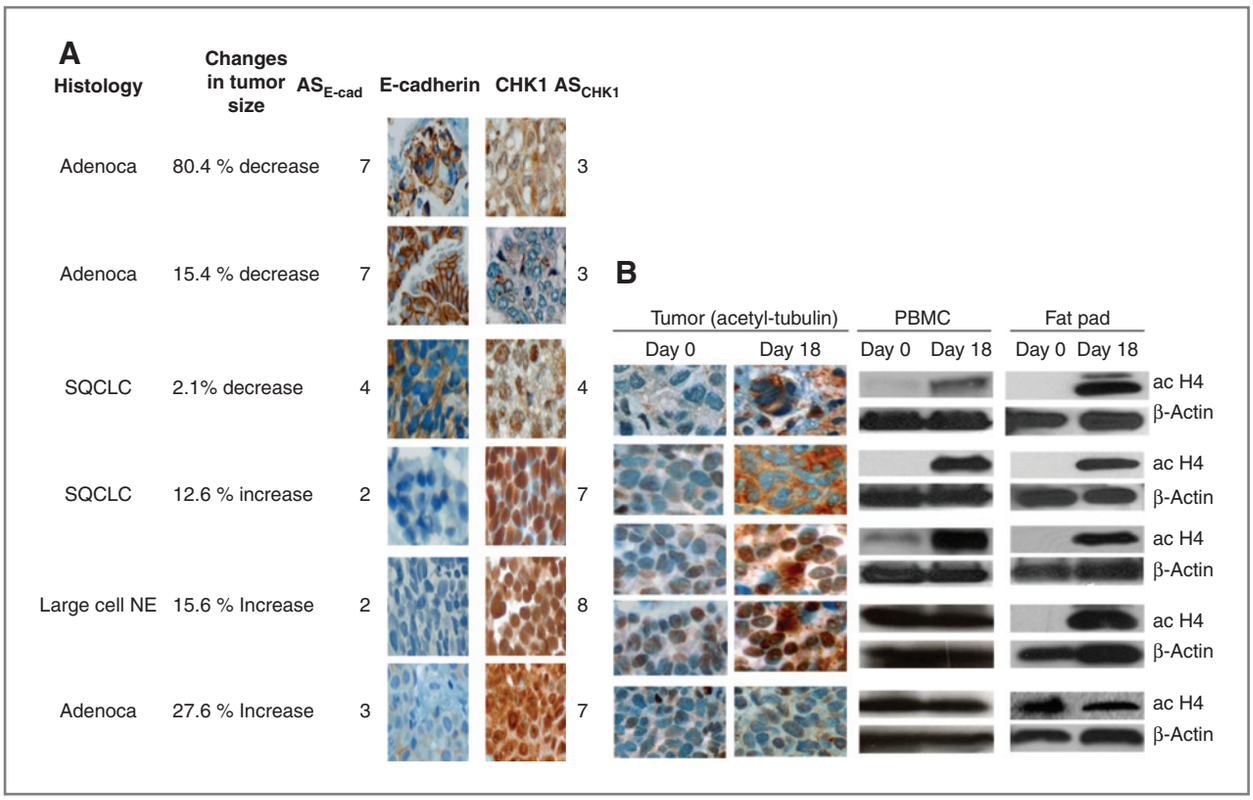

Figure 4. A, CHK1 score inversely correlates with E-cadherin expression, percentage decrease in tumor size, and PFS in NSCLC. Adenoca, adenocarcinoma; Large cell NE, large cell neuroendocrine carcinoma; AS, Allred score. B, panobinostat plus erlotinib therapy induces tubulin acetylation in tumor cells as well as histone H4 acetylation (ac H4) in subcutaneous fat tissue and PBMC, as assessed by Western blot analysis. β-Actin was used as a loading control.

mediated cytotoxicity in NSCLC cells (16, 27), in which overexpression of CHK1 leads to resistance to HDAC inhibitors, including panobinostat. We investigated whether percentage change in tumor size to panobinostat and erlotinib correlated with CHK1 expression by immunohistochemistry analysis on pretreatment tumor tissue available from 6 patients participating in this trial. As shown in Fig. 4A, CHK1 was highly expressed in the nuclei and cytoplasm of tumors that showed progressive disease, whereas its expression was lowest in those with tumor shrinkage, two lung adenocarcinomas and one SQCLC. No changes were observed in the CHK1 expression in pre and post treatment biopsy samples (data not shown). A strong negative correlation was observed between CHK1 score and percentage decrease in tumor size ($P = 0.02$) and PFS ($P = 0.006$).

Previous studies have shown that high E-cadherin expression levels confer increased sensitivity to HDAC inhibitor + EGFR-TKI combination treatment in NSCLC (19, 28). We evaluated E-cadherin expression in pretreatment tumor tissues and related this to response and CHK1. As illustrated in Fig. 4A, E-cadherin score was marginally associated with percentage change in tumor size ($P = 0.06$). Tumors that showed increased tumor size expressed low to no E-cadherin, whereas tumors with the highest levels of E-cadherin expression had the greatest decrease in tumor size. We also showed that E-cadherin expression positively correlated with PFS ($P = 0.02$). Furthermore, CHK1 score and E-cadherin expression showed a strong negative correlation ($P = 0.003$).

Adipose tissue as surrogate target for HDAC inhibitor therapy

In preclinical studies, we have previously demonstrated that fat tissue obtained from patients by fine needle aspiration (FNA) biopsy of the subcutaneous adipose tissue can be used to detect the activity of signaling pathways and histone acetylation, suggesting that the subcutaneous fat pad might serve as a surrogate tissue to assess the efficacy of the HDAC inhibitors *in vivo* (29). We collected pre and posttreatment abdominal FPBs, and treatment effect was measured as change in the activity of acetylation of histone H4 in 17 matching FPB and PBMC samples. An increase in H4 acetylation was observed in 8 PBMC samples and in 10 FPB samples, 7 of which overlapped. No change in acetyl-H4 levels was observed in 9 PBMC samples and 7 patients with FPBs, 5 of which overlapped. Figure 4B illustrates a representation of 5 matching tumor, PBMC, and FPBs. In 4 patients, the pre and posttreatment levels of acetyl-tubulin in tumor tissue closely correlated with the levels of histone acetylation in PBMC and in fat pad samples, and, in one patient increased acetyl-tubulin in tumor tissue correlated with increased acetyl-histone levels only in fat pad but not

Published OnlineFirst January 15, 2014; DOI: 10.1158/1078-0432.CCR-13-2235

in PBMC samples. Furthermore, our results showed that in 67% (8 of 12) of patients with clinical response of stable disease and PR, there was increased histone acetylation in fat pad samples, whereas only 36% patients (4 of 11) in this response category showed increased histone acetylation in PBMC. In both sample types, there was increased histone acetylation in 1 of 3 patients with the clinical response of PD. These results suggest that histone acetylation in fat pad likely correlates with changes in tumor size in patients treated with HDAC inhibitors; however, additional clinical studies with larger sample size are needed to better understand the correlation between fat pad histone acetylation and clinical response to HDAC inhibitor treatment.

Discussion

In this study, we established the MTD of panobinostat to be 30 mg *per os* twice weekly, for 2 out of 3 weeks of each cycle, in combination with erlotinib at 100 mg *per os* daily. At the MTD/RP2D, the combination was a well tolerated in patients with NSCLC or head and neck cancer. The main adverse events were fatigue, nausea, rash, and thrombocytopenia. Prolonged QTc and nausea led to a DLT in the DL3 cohort. No new adverse events were revealed compared with that shown in prior single-agent studies of erlotinib (18) and panobinostat (13). The pharmacokinetic parameters for erlotinib and panobinostat (14) seen in this study are consistent with the previously reported literature.

Our overall DCR of 52% among evaluable patients was comparable with prior studies that only enrolled erlotinib-naïve patients (18). This is of interest as the study included patients who progressed on prior erlotinib. In the NSCLC *EGFR*-mutant group, the median OS in these previously treated patients, including 4 patients with prior erlotinib treatment (mean number of lines of prior therapy was 2.3), was estimated to be 41 months. Prospective randomized trials evaluating patients with *EGFR*-mutant NSCLC treated with first-line single-agent EGFR-TKIs have demonstrated an OS of 19.3 to 30.9 months (30–32). Despite the *post hoc* nature of the analysis, small sample size, reference to historic controls, and exclusion of patients with NSCLC with *EGFR* unknown status, our findings are in line with a previous report that included patients with known *EGFR* status (28).

All responses were among *EGFR*-mutant, EGFR-TKI–naïve patients. Among all NSCLC groups evaluated, whether *EGFR*-mutant, *EGFR* wild-type, or *EGFR* unknown, those who were EGFR-TKI naïve were more likely to benefit from the combination treatment than those with prior EGFR-TKI exposure. Still, radiographic and meaningful clinical benefits were observed in those with prior exposure to EGFR-TKI, including a patient with EGFR wild-type lung adenocarcinoma who was a lifetime never-smoker with a near PR following treatment with the combination treatment.

In the preclinical setting, HDAC inhibitors can eradicate and prevent drug-tolerant populations (21) and have shown activity against EGFR-TKI–resistant NSCLC cell lines (8, 19). Treatment with HDAC inhibitors may reverse or prevent drug resistance to EGFR-TKIs, and this could in part explain the study observations. HDAC inhibitors have broad mechanisms of action, as they affect the expression of numerous genes involved in apoptosis (33), angiogenesis (10), immune response (34, 35), and tumor growth inhibition (4). Because of a host of complex epigenetic activities leading to direct and indirect inhibitor effects, within a clinical setting, the precise actions of HDAC inhibitors have proven challenging to illuminate and are likely multifactorial. Other factors may also play a role. Retrospective studies have demonstrated the potential benefit of re-treatment or continuation treatment with single agent EGFR-TKI in patients post progression (36–41). Further clinical and preclinical studies are required to better elucidate the clinical benefit and refine time to resistance of erlotinib and panobinostat in patients with *EGFR*-mutant NSCLC.

Published studies have demonstrated the feasibility of erlotinib, alone or in combination with a rexinoid or chemotherapy in patients with metastatic or refractory head and neck cancer (42–44). These studies also demonstrate the rationale behind the use of erlotinib in patients with head and neck cancer, although it is not indicated by the FDA. Because patients with head and neck cancer have limited options in the salvage setting, our findings are of interest, despite our limited sample size. Three of the 7 evaluable patients with head and neck cancer achieved stable disease. These included 1 who received nine cycles of therapy and another patient treated for six cycles before progression. Interestingly, we observed that those with head and neck cancer achieved a higher DCR (43%) and OS (8.2 months) than patients with SQCLC of the lung (DCR = 14%; OS = 5.5 months).

We observed that high E-cadherin expression levels correlated with improved outcomes independent of *EGFR* mutation status and tumor histology. Prior studies have demonstrated that epithelial–mesenchymal transition results in acquired resistance to EGFR-TKIs in patients with *EGFR* mutation (41, 45, 46) and that high E-cadherin expression (a marker of epithelial phenotype) correlates with EGFR-TKI activity (47–49). In a recent clinical trial, E-cadherin expression has been shown to predict response to EGFR-TKI and HDAC inhibitor combination in patients with NSCLC. Here, we also observed a strong negative correlation between CHK1 immunohistochemistry score and E-cadherin expression, PFS, and percentage decrease in tumor size with statistical significance. This finding is consistent with our preclinical data (16), in which we found that overexpression of CHK1 led to resistance to panobinostat. Despite the small sample size, our results suggest that expression levels of high E-cadherin plus low CHK1 in tumor tissue might indicate a favorable outcome and may help to identify subgroups of patients with NSCLC to determine tumor sensitivity or resistance at the early stages of therapy.

Attempts to establish a correlation between surrogate markers such as histone hyperacetylation in PBMCs and drug efficacy in tumor tissue are not always consistent with measured pharmacokinetic profiles of HDAC inhibitors, as

Published OnlineFirst January 15, 2014; DOI: 10.1158/1078-0432.CCR-13-2235

findings can vary from patient to patient (50) and data interpretation poses challenges in the setting of background noise (51). The reasons why PBMCs differ from tumor tissue in their response to HDAC inhibitors are not completely understood and could be related to insufficient drug penetration, particularly in solid tumors due to differences in tissue architecture and hemodynamics. In addition, PBMCs are a mixed population of T cells, B cells, monocytes, and natural killer cells, and it has been shown that each individual cell population contributes differently to the histone acetylation detected after treatment with HDAC inhibitor (51), indicating that histone acetylation levels in PBMCs after treatment with an HDAC inhibitor might not be directly comparable across patients. In this study, we hypothesized that given its homogeneity, mature adipose tissue might be an appropriate surrogate tissue to assess the pharmacodynamic efficacy of HDAC inhibitor treatment that would allow direct comparison of drug response across patients and studies. Abdominal FPB is a minimally invasive and well-established routine diagnostic method for amyloid detection (52, 53) that can provide highly cellular samples to perform correlative studies. Given the abundance and easy accessibility, fat tissue allows repeated sampling during the course of therapy to monitor the efficacy of HDAC inhibitor treatment. To our knowledge, we show here for the first time that serial fat pad FNA biopsy sampling can be used to monitor the efficacy of HDAC inhibitors *in vivo*. Correlation of the degree of induction of histone acetylation in fat pad samples and inhibition of HDAC activity in tumor tissue showed the applicability of fat tissue as a surrogate of HDAC inhibitor response. Whether a correlation between the HDAC enzyme activity in fat pad and the therapeutic response exists needs to be determined in future studies. Documentation of drug-mediated changes in the activity of signaling pathways in fat cells also suggests that fat tissue could be used as a surrogate to monitor the efficacy of other targeted drugs in future clinical studies. With more than 100 current studies evaluating HDAC inhibitors (clinicaltrials.gov), our assessment of FPB is relevant.

In summary, we provide evidence that erlotinib plus panobinostat is a tolerable combination in patients with advanced NSCLC and head and neck cancer. The potential benefit of this combination in the *EGFR*-mutant population and evidence of activity in a population with acquired resistance to erlotinib are intriguing and require additional studies. Although our sample size is small, the data presented here suggest that fat pad tissue obtained by FNA may have application in monitoring the *in vivo* efficacy of HDAC inhibitors. Our correlative data lay the foundation for a biomarker-driven clinical trial to confirm these findings, to investigate fat pad FNA biopsy, and to validate the predictive role of CHK1 expression in response to treatments involving HDAC inhibitors.

Disclosure of Potential Conflicts of Interest

A. Chiappori has honoraria from Celgene, Genentech, and Pfizer, and is consultant/advisory board member for Novartis. M. Pinder-Schenck has received honoraria from Genentech. No potential conflicts of interest were disclosed by the other authors.

Authors' Contributions

Conception and design: J.E. Gray, E. Haura, R. Lush, M.J. Schell, G. Bepler, S. Altiok
Development of methodology: J.E. Gray, A. Neuger, S. Altiok
Acquisition of data (provided animals, acquired and managed patients, provided facilities, etc.): J.E. Gray, E. Haura, A. Chiappori, T. Tanvetyanon, C.C. Williams, M. Pinder-Schenck, J. Kreahling, A. Neuger, L. Tetteh, A. Akar, G. Bepler, S. Altiok
Analysis and interpretation of data (e.g., statistical analysis, biostatistics, computational analysis): J.E. Gray, E. Haura, J. Kreahling, R. Lush, A. Neuger, X. Zhao, M.J. Schell, G. Bepler, S. Altiok
Writing, review, and/or revision of the manuscript: J.E. Gray, E. Haura, A. Chiappori, T. Tanvetyanon, C.C. Williams, M. Pinder-Schenck, R. Lush, A. Neuger, X. Zhao, M.J. Schell, G. Bepler, S. Altiok
Administrative, technical, or material support (i.e., reporting or organizing data, constructing databases): J.E. Gray, R. Lush, L. Tetteh, A. Akar, S. Altiok
Study supervision: J.E. Gray, E. Haura, S. Altiok
Contribution of patients for the study: J.A. Kish

Acknowledgments

The authors thank Rasa Hamilton (H. Lee Moffitt Cancer Center) for editorial assistance.

Grant Support

The study was sponsored by Novartis Pharmaceuticals and Genentech. This work was also supported in part by the National Cancer Institute, part of the NIH, through grant number P30-CA76292-14 and R21-CA123888.

The costs of publication of this article were defrayed in part by the payment of page charges. This article must therefore be hereby marked *advertisement* in accordance with 18 U.S.C. Section 1734 solely to indicate this fact.

Received August 13, 2013; revised December 4, 2013; accepted December 19, 2013; published OnlineFirst January 15, 2014.

References

1. Marks P, Rifkind RA, Richon VM, Breslow R, Miller T, Kelly WK. Histone deacetylases and cancer: causes and therapies. Nat Rev Cancer 2001;1:194–202.
2. Marks PA, Dokmanovic M. Histone deacetylase inhibitors: discovery and development as anticancer agents. Expert Opin Investig Drugs 2005;14:1497–511.
3. Cress WD, Seto E. Histone deacetylases, transcriptional control, and cancer. J Cell Physiol 2000;184:1–16.
4. Glozak MA, Sengupta N, Zhang X, Seto E. Acetylation and deacetylation of non-histone proteins. Gene 2005;363:15–23.
5. Kim SC, Sprung R, Chen Y, Xu Y, Ball H, Pei J, et al. Substrate and functional diversity of lysine acetylation revealed by a proteomics survey. Mol Cell 2006;23:607–18.
6. Lane AA, Chabner BA. Histone deacetylase inhibitors in cancer therapy. J Clin Oncol 2009;27:5459–68.
7. Yang XJ, Seto E. Lysine acetylation: codified crosstalk with other posttranslational modifications. Mol Cell 2008;31:449–61.
8. Edwards A, Li J, Atadja P, Bhalla K, Haura E. Effect of the histone deacetylase inhibitor LBH589 against epidermal growth factor receptor-dependant human lung cancer cells. Mol Cancer Ther 2007;6:1–10.
9. Crisanti MC, Wallace AF, Kapoor V, Vandermeers F, Dowling ML, Pereira LP, et al. The HDAC inhibitor panobinostat (LBH589) inhibits mesothelioma and lung cancer cells *in vitro* and *in vivo* with particular efficacy for small cell lung cancer. Mol Cancer Ther 2009;8:2221–31.

Published OnlineFirst January 15, 2014; DOI: 10.1158/1078-0432.CCR-13-2235

10. Qian DZ, Kato Y, Shabbeer S, Wei Y, Verheul HM, Salumbides B, et al. Targeting tumor angiogenesis with histone deacetylase inhibitors: the hydroxamic acid derivative LBH589. Clin Cancer Res 2006;12:634–42.
11. Floris G, Debiec-Rychter M, Sciot R, Stefan C, Fieuws S, Machiels K, et al. High efficacy of panobinostat towards human gastrointestinal stromal tumors in a xenograft mouse model. Clin Cancer Res 2009;15:4066–76.
12. Heider U, Kaiser M, Sterz J, Zavrski I, Jakob C, Fleissner C, et al. Histone deacetylase inhibitors reduce VEGF production and induce growth suppression and apoptosis in human mantle cell lymphoma. Eur J Haematol 2006;76:42–50.
13. Giles F, Fischer T, Cortes J, Garcia-Manero G, Beck J, Ravandi F, et al. A phase I study of intravenous LBH589, a novel cinnamic hydroxamic acid analogue histone deacetylase inhibitor, in patients with refractory hematologic malignancies. Clin Cancer Res 2006;12:4628–35.
14. Rathkopf D, Wong BY, Ross RW, Anand A, Tanaka E, Woo MM, et al. A phase I study of oral panobinostat alone and in combination with docetaxel in patients with castration-resistant prostate cancer. Cancer Chemother Pharmacol 2010;66:181–9.
15. Bartek J, Lukas J. Chk1 and Chk2 kinases in checkpoint control and cancer. Cancer Cell 2003;3:421–9.
16. Brazelle W, Kreahling JM, Gemmer J, Ma Y, Cress WD, Haura E, et al. Histone deacetylase inhibitors downregulate checkpoint kinase 1 expression to induce cell death in non-small cell lung cancer cells. PLoS ONE 2010;5:e14335.
17. Pao W, Miller VA. Epidermal growth factor receptor mutations, small-molecule kinase inhibitors, and non-small-cell lung cancer: current knowledge and future directions. J Clin Oncol 2005;23:2556–68.
18. Shepherd FA, Rodrigues Pereira J, Ciuleanu T, Tan EH, Hirsh V, Thongprasert S, et al. Erlotinib in previously treated non-small-cell lung cancer. N Engl J Med 2005;353:123–32.
19. Witta SE, Gemmill RM, Hirsch FR, Coldren CD, Hedman K, Ravdel L, et al. Restoring E-cadherin expression increases sensitivity to epidermal growth factor receptor inhibitors in lung cancer cell lines. Cancer Res 2006;66:944–50.
20. Ozaki K, Kosugi M, Baba N, Fujio K, Sakamoto T, Kimura S, et al. Blockade of the ERK or PI3K-Akt signaling pathway enhances the cytotoxicity of histone deacetylase inhibitors in tumor cells resistant to gefitinib or imatinib. Biochem Biophys Res Commun 2010;391:1610–5.
21. Sharma SV, Lee DY, Li B, Quinlan MP, Takahashi F, Maheswaran S, et al. A chromatin-mediated reversible drug-tolerant state in cancer cell subpopulations. Cell 2010;141:69–80.
22. Gao YS, Hubbert CC, Lu J, Lee YS, Lee JY, Yao TP. Histone deacetylase 6 regulates growth factor-induced actin remodeling and endocytosis. Mol Cell Biol 2007;27:8637–47.
23. Gao YS, Hubbert CC, Yao TP. The microtubule-associated histone deacetylase 6 (HDAC6) regulates epidermal growth factor receptor (EGFR) endocytic trafficking and degradation. J Biol Chem 2010;285:11219–26.
24. Lepper ER, Swain SM, Tan AR, Figg WD, Sparreboom A. Liquid-chromatographic determination of erlotinib (OSI-774), an epidermal growth factor receptor tyrosine kinase inhibitor. J Chromatogr B Analyt Technol Biomed Life Sci 2003;796:181–8.
25. Zhao M, He P, Rudek MA, Hidalgo M, Baker SD. Specific method for determination of OSI-774 and its metabolite OSI-420 in human plasma by using liquid chromatography-tandem mass spectrometry. J Chromatogr B Analyt Technol Biomed Life Sci 2003;793:413–20.
26. Hamberg P, Woo MM, Chen LC, Verweij J, Porro MG, Zhao L, et al. Effect of ketoconazole-mediated CYP3A4 inhibition on clinical pharmacokinetics of panobinostat (LBH589), an orally active histone deacetylase inhibitor. Cancer Chemother Pharmacol 2011;68:805–13.
27. Noh EJ, Lim DS, Jeong G, Lee JS. An HDAC inhibitor, trichostatin A, induces a delay at G2/M transition, slippage of spindle checkpoint, and cell death in a transcription-dependent manner. Biochem Biophys Res Commun 2009;378:326–31.
28. Witta SE, Jotte RM, Konduri K, Neubauer MA, Spira AI, Ruxer RL, et al. Randomized phase II trial of erlotinib with and without entinostat in patients with advanced non-small-cell lung cancer who progressed on prior chemotherapy. J Clin Oncol 2012;30:2248–55.
29. Altiok S, Brazelle W, Gemmer J, Haura E. Subcutaneous adipose tissue as a surrogate for pharmacodynamic assessment of HDAC inhibitors. In: Proceedings of the ASCO Molecular Markers Meeting; 2008; Abstract nr 123.
30. Maemondo M, Inoue A, Kobayashi K, Sugawara S, Oizumi S, Isobe H, et al. Gefitinib or chemotherapy for non-small-cell lung cancer with mutated EGFR. N Engl J Med 2010;362:2380–8.
31. Mitsudomi T, Morita S, Yatabe Y, Negoro S, Okamoto I, Tsurutani J, et al. Gefitinib versus cisplatin plus docetaxel in patients with non-small-cell lung cancer harbouring mutations of the epidermal growth factor receptor (WJTOG3405): an open label, randomised phase 3 trial. Lancet Oncol 2010;11:121–8.
32. Rosell R, Carcereny E, Gervais R, Vergnenegre A, Massuti B, Felip E, et al. Erlotinib versus standard chemotherapy as first-line treatment for European patients with advanced EGFR mutation-positive non-small-cell lung cancer (EURTAC): a multicentre, open-label, randomised phase 3 trial. Lancet Oncol 2012;13:239–46.
33. Moore PS, Barbi S, Donadelli M, Costanzo C, Bassi C, Palmieri M, et al. Gene expression profiling after treatment with the histone deacetylase inhibitor trichostatin A reveals altered expression of both pro- and anti-apoptotic genes in pancreatic adenocarcinoma cells. Biochim Biophys Acta 2004;1693:167–76.
34. Khan AN, Tomasi TB. Histone deacetylase regulation of immune gene expression in tumor cells. Immunol Res 2008;40:164–78.
35. Bridle BW, Chen L, Lemay CG, Diallo JS, Pol J, Nguyen A, et al. HDAC inhibition suppresses primary immune responses, enhances secondary immune responses, and abrogates autoimmunity during tumor immunotherapy. Mol Ther 2013;21:887–94.
36. Chaft JE, Oxnard GR, Sima CS, Kris MG, Miller VA, Riely GJ. Disease flare after tyrosine kinase inhibitor discontinuation in patients with EGFR-mutant lung cancer and acquired resistance to erlotinib or gefitinib: implications for clinical trial design. Clin Cancer Res 2011;17:6298–303.
37. Goldberg SB, Oxnard GR, Digumarthy S, Muzikansky A, Jackman DM, Lennes IT, et al. Chemotherapy with erlotinib or chemotherapy alone in advanced non-small cell lung cancer with acquired resistance to EGFR tyrosine kinase inhibitors. Oncologist 2013;18:1214–20.
38. Heon S, Nishino M, Goldberg SB, Porter J, Sequist LV, Jackman DM, et al. Response to EGFR tyrosine kinase inhibitor (TKI) retreatment after a drug-free interval in EGFR-mutant advanced non-small cell lung cancer (NSCLC) with acquired resistance. J Clin Oncol 30, 2012 (suppl; abstr 7525).
39. Oxnard GR, Janjigian YY, Arcila ME, Sima CS, Kass SL, Riely GJ, et al. Maintained sensitivity to EGFR tyrosine kinase inhibitors in EGFR-mutant lung cancer recurring after adjuvant erlotinib or gefitinib. Clin Cancer Res 2011;17:6322–8.
40. Oxnard GR, Lo P, Jackman DM, Butaney M, Heon S, Johnson BE, et al. Delay of chemotherapy through use of post-progression erlotinib in patients with EGFR-mutant lung cancer. J Clin Oncol 30, 2012 (suppl; abstr 7547).
41. Sequist LV, Waltman BA, Dias-Santagata D, Digumarthy S, Turke AB, Fidias P, et al. Genotypic and histological evolution of lung cancers acquiring resistance to EGFR inhibitors. Sci Transl Med 2011;3:75ra26.
42. Dragnev KH, Petty WJ, Shah S, Biddle A, Desai NB, Memoli V, et al. Bexarotene and erlotinib for aerodigestive tract cancer. J Clin Oncol 2005;23:8757–64.
43. Siu LL, Soulieres D, Chen EX, Pond GR, Chin SF, Francis P, et al. Phase I/II trial of erlotinib and cisplatin in patients with recurrent or metastatic squamous cell carcinoma of the head and neck: a Princess Margaret Hospital phase II consortium and National Cancer Institute of Canada Clinical Trials Group Study. J Clin Oncol 2007;25:2178–83.
44. Soulieres D, Senzer NN, Vokes EE, Hidalgo M, Agarwala SS, Siu LL. Multicenter phase II study of erlotinib, an oral epidermal growth factor receptor tyrosine kinase inhibitor, in patients with recurrent or metastatic squamous cell cancer of the head and neck. J Clin Oncol 2004;22:77–85.
45. Uramoto H, Iwata T, Onitsuka T, Shimokawa H, Hanagiri T, Oyama T. Epithelial-mesenchymal transition in EGFR-TKI acquired resistant lung adenocarcinoma. Anticancer Res 2010;30:2513–7.

Published OnlineFirst January 15, 2014; DOI: 10.1158/1078-0432.CCR-13-2235

46. Chung JH, Rho JK, Xu X, Lee JS, Yoon HI, Lee CT, et al. Clinical and molecular evidences of epithelial to mesenchymal transition in acquired resistance to EGFR-TKIs. Lung Cancer 2011;73:176–82.

47. Yauch RL, Januario T, Eberhard DA, Cavet G, Zhu W, Fu L, et al. Epithelial versus mesenchymal phenotype determines *in vitro* sensitivity and predicts clinical activity of erlotinib in lung cancer patients. Clin Cancer Res 2005;11:8686–98.

48. Thomson S, Buck E, Petti F, Griffin G, Brown E, Ramnarine N, et al. Epithelial to mesenchymal transition is a determinant of sensitivity of non-small-cell lung carcinoma cell lines and xenografts to epidermal growth factor receptor inhibition. Cancer Res 2005;65:9455–62.

49. Coldren CD, Helfrich BA, Witta SE, Sugita M, Lapadat R, Zeng C, et al. Baseline gene expression predicts sensitivity to gefitinib in non-small cell lung cancer cell lines. Mol Cancer Res 2006;4:521–8.

50. Ryan QC, Headlee D, Acharya M, Sparreboom A, Trepel JB, Ye J, et al. Phase I and pharmacokinetic study of MS-275, a histone deacetylase inhibitor, in patients with advanced and refractory solid tumors or lymphoma. J Clin Oncol 2005;23:3912–22.

51. Novotny-Diermayr V, Sausgruber N, Loh YK, Pasha MK, Jayaraman R, Hentze H, et al. Pharmacodynamic evaluation of the target efficacy of SB939, an oral HDAC inhibitor with selectivity for tumor tissue. Mol Cancer Ther 2011;10:1207–17.

52. van G II, Hazenberg BP, Bijzet J, van Rijswijk MH. Diagnostic accuracy of subcutaneous abdominal fat tissue aspiration for detecting systemic amyloidosis and its utility in clinical practice. Arthritis Rheum 2006;54:2015–21.

53. van G II, Hazenberg BP, Bijzet J, Haagsma EB, Vellenga E, Posthumus MD, et al. Amyloid load in fat tissue reflects disease severity and predicts survival in amyloidosis. Arthritis Care Res 2010;62:296–301.

Published OnlineFirst January 15, 2014; DOI: 10.1158/1078-0432.CCR-13-2235

AACR American Association for Cancer Research

Clinical Cancer Research

A Phase I, Pharmacokinetic, and Pharmacodynamic Study of Panobinostat, an HDAC Inhibitor, Combined with Erlotinib in Patients with Advanced Aerodigestive Tract Tumors

Jhanelle E. Gray, Eric Haura, Alberto Chiappori, et al.

Clin Cancer Res 2014;20:1644-1655. Published OnlineFirst January 15, 2014.